2020-12-01

Intention recognition of elbow joint based on sEMG using adaptive fuzzy neural network

Liu, Y

http://hdl.handle.net/10026.1/17240

10.1109/ICMCCE51767.2020.00240
Proceedings - 2020 5th International Conference on Mechanical, Control and Computer Engineering, ICMCCE 2020

Intention Recognition of Elbow Joint based on sEMG Using Adaptive Fuzzy Neural Network

Conference Paper · December 2020

DOI: 10.1109/ICMCCE51767.2020.00240

Intention Recognition of Elbow Joint based on sEMG Using Adaptive Fuzzy Neural Network

Yongbai Liu
Department of Control Engineering
Changchun University of Technology
Changchun, China
2201804053@stu.ccut.edu.cn

Zhaowei Teng
Department of Control Engineering
Changchun University of Technology
Changchun, China
1141063356@qq.com

Gang Wang
Department of Control Engineering
Changchun University Of Technology
Changchun, China
wg960109@163.com

Chunxu Li
Centre for Robotics and Neural Systems
University of Plymouth
Plymouth, UK
chunxu.li@plymouth.ac.uk

Keping Liu
Department of Control Engineering
Changchun University of Technology
Changchun, China
liukeping@ccut.edu.cn

Zhongbo Sun*
Department of Control Engineering
Changchun University of Technology
Changchun, China
zhongbosun2012@163.com

***Abstract*— In this paper, the adaptive fuzzy neural network (AFNN) based on the surface electromyography (sEMG) for estimating the elbow joint angle is established and investigated from the perspective of rapidity and accuracy. In addition, back propagation neural network (BPNN) and artificial neural network of radial basis function (RBFNN), as the classical method for data forecasting, have been applied to estimate the elbow joint angle for comparing with AFNN. Ultimately, the experimental simulation and result analysis demonstrate that the rapidity and accuracy of AFNN is superior to BPNN and RBFNN.**

Keywords-Adaptive fuzzy neural network, sEMG signal, RMS error, Intention recognition, Rehabilitation

I. INTRODUCTION

With the aging of China's population, the number of limb disabilities caused by stroke, spinal cord injury, brain trauma and other reasons are increasing rapidly. Among them, stroke is the main disease that causes local skeletal muscle dysfunction in people's upper limbs, and most patients have a certain degree of dysfunction. Stroke disease has the characteristics of high disability rate, obvious younger trend, and great harm, which seriously endangers the physical and mental health of patients, and also brings a heavy economic burden to the patient's family and society [1]. Therefore, the most important thing is to take necessary measures to help patients with physical disabilities get rehabilitation treatment. The traditional rehabilitation training method is mainly artificial or simple equipment to drive the affected limb to perform rehabilitation training activities. This rehabilitation training method generally requires the assistance of multiple medical staff. However, the medical staff has a problem of heavy physical exertion and it is difficult to ensure the intensity of the rehabilitation training and persistence. Therefore, the traditional rehabilitation treatment methods have disadvantages such as high personnel consumption, long recovery period, and limited effects. However, with the rapid development of robots in the medical, military, industrial and other neighborhoods [2-4]. Compared with traditional rehabilitation treatment, the application of upper limb rehabilitation robots to assist patients in rehabilitation training activities will be a more convenient, practical and superior training method. Therefore, intention recognition technology, a core technique in the field of rehabilitation robot research, will become an important part of the human-computer interactive control of rehabilitation robots [5-6].

Human motion intentions are generated in the brain, and conveyed to joint motion through multiple complex neural subsystems. In addition, the surface biological signals, which are usually applied in rehabilitation robot applications to reflect the intention of human movement. Therefore, it requires the upper limb rehabilitation robots to measure and collect the human body's biological signals and accurately identify human motion intentions. At present, biological signals mainly comprise electroencephalogram (EEG), electrooculogram (EOG), electromyography (EMG) and mechanical signals etc. [2], [7], [8]. In recent years, with the widespread application of neural networks in the fields of science and engineering [9]-[11], domestic and foreign scholars have proposed a variety of schemes, such as support vector machine (SVM) [12], artificial neural networks [13], BPNN [14] and RBFNN [15] etc, to estimate the joint angle from the surface biological signals, so as to realize the recognition of the human body intention. Specifically, In [16], Y.Masahiro et al. proposed a continuous hand pose estimation method, which is based on the SVM and relationship between EMG signal and joint angle, and the experiments show a high accuracy rate for motion classification and joint angle estimation. In [14], Zhang et al. applied the BPNN to realize the joint angle estimation of hip, knee and ankle via the surface electromyographic signals of different muscles. Simultaneously, the parameters discussion ensures that the RMS error of intention recognition is minimized under the optimal parameters. In addition, in [15], the RBFNN was utilized to estimate the joint angles of hip, knee, and ankle from the sEMG signals of rectus femoris, lateral femoral muscle and extensor halluces. The RMS error of intention recognition reached a controllable range. Meanwhile, in [17], Li et al. designed the iterative learning controller based on the RBFNN, which accomplished the intention recognition of lower limbs, to realize the gait tracking of the lower limb rehabilitation robot under the condition of noise pollution. In [18], a long short term memory network (LSTM) has been applied by Chai et al. to estimate the elbow joint angle from the sEMG signals. Although numerous algorithms have been developed, analyzed

The work is supported in part by the National Natural Science Foundation of China under grants 61873304, and in part by the China Postdoctoral Science Foundation Funded Project under grant 2018M641784, 2019T120240 and also in part by the Key Science and Technology Projects of Jilin Province, China, grant nos. 20200201291JC.

978-1-6654-2314-4/20/$31.00 ©2020 IEEE
DOI 10.1109/ICMCCE51767.2020.00240

and investigated for human intention recognition based on the sEMG signals, the accuracy, rapidity and stability of the algorithm still have a crucial significance in the research of human intention recognition. The algorithms with the ability of high-precision, robustness and real-time will facilitate the application of rehabilitation robots in the fields of limb rehabilitation.

In this paper, the AFNN based on the sEMG signals, is developed and applied to estimate the elbow joint angle in the human intention recognition. Specifically, the sEMG signal of biceps muscle will be collected by the equipment of biopac system MP160. Meanwhile, the actual angle of elbow joint will be gathered by the WT901C485 angle sensor. In order to obtain the mainly characteristics of the human sEMG signal, then, the raw sEMG signals need to be processed by high-pass filter and low-pass filter to remove the polluted signals. For comparison, the BPNN and RBFNN will also be utilized to estimate the joint angle of the upper limb elbow joint. Ultimately, the experimental results prove that AFNN is superior to the BPNN and RBFNN in terms of accuracy and rapidity in human intention recognition.

The remainder of this paper is organized as follows. In Section II, there are two parts of data acquisition and signal processing. The establishment of AFNN model is introduced in Section III, including the structure diagram and flowchart of AFNN. Then, in order to demonstrate the superior performance of the AFNN model, the experiment simulation and comparison experiments are carried out in Section IV. In the end, Section V concludes the future works of this paper. The main contributions of this paper are as follows.

- An innovative method AFNN is proposed for human intention recognition of upper limb elbow joint in this paper.
- Experimental simulation and model comparison, which demonstrate that the superior performance of the AFNN model in the estimation of elbow joint angle.

II. EXPERIMENTAL METHODS

A. Data acquisition

In this experiment, a able-bodied test subject (male, 27 years old, 172cm, 84kg), take part in the experiment of arm flexion and extension. On account of the movement of the elbow joint mainly depends on the flexion and extension of the biceps, then, the electrodes will be attached on the surface of biceps muscle. Specifically, the WT901C485 angle sensor and biopac system MP160 are shown in Fig. 1 (a) and Fig. 1 (b), and the procedures of this experiment are introduced as follows:

(a)

(b)

Fig. 1. The WT901C485 angle sensor and biopac system MP160. (a) WT901C485 angle sensor. (b) Biopac system MP160.

- Cleaning the surface of biceps muscle with alcohol and attaching three electrode slices to it. Specially, the distance between each electrode slice is 2cm-3cm.
- Binding the WT901C485 angle sensor and the Biopac signal transmission module to the subject's upper arm and connecting the wireless transmitting module and receiving module.
- Applying the computer software MiniIMU and Acp-Knowledge 5.0 for data acquisition.

Following the above data acquisition steps, as shown in Fig. 3, the raw sEMG signals are collected in 80s with the 2KHZ sampling rate. As revealed in Fig. 4, the WT901C485 angle sensor obtains the elbow joint angle with the 100HZ sampling rate. In addition, for the reader's convenience, the installation location of WT901C485 angle sensor, biopac signal transmission module and experimental environment are shown in Fig. 2.

B. Signals processing

It can be seen from Fig. 3 and Fig. 4 that the test subject achieves 8-9 cycles in 80s, However, the raw sEMG signals of biceps muscle are polluted by noises in the process of data acquisition. Specifically, there are many noises from the equipments of WT901C485 and MP160, electromagnetic and test environment, including 50Hz industrial frequency noise, DC bias, sweat and temperature and so on.

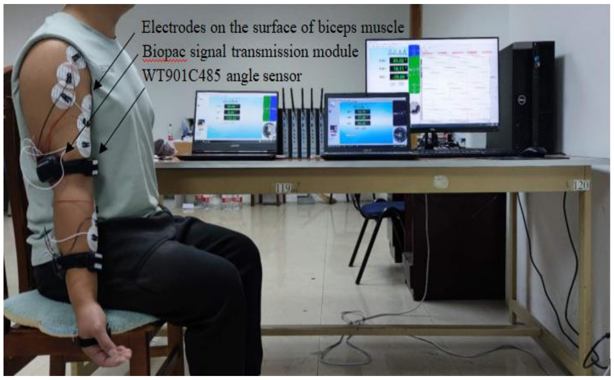

Fig. 2. The experimental environment during the data acquisition.

In order to obtain the major characteristic of raw sEMG signals of biceps muscle, the frequency of 0-500Hz needs to be filtered [19]. In addition, the low frequency 20HZ and 50HZ should be cut-off by reason of the industrial frequency of 50 HZ and motor unit frequency 20HZ [20]. In conclusion, a 500HZ high-pass filter, 20HZ low-pass filter and 50HZ notch filter are applied to wipe off the invalid frequency information in the processing of raw sEMG signal.

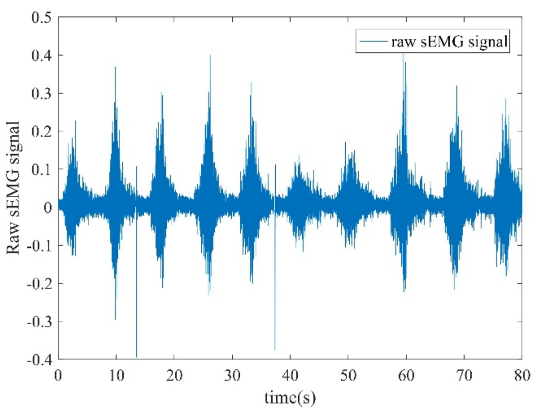

Fig. 3. The raw sEMG signal of biceps muscle collected in the data acquisition.

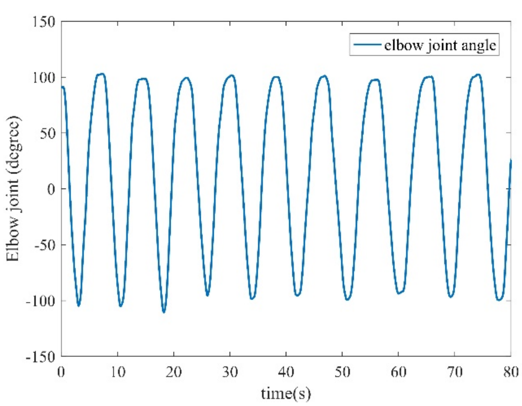

Fig. 4. The actual elbow joint angle recorded in the data acquisition.

As a consequence, the processed signal $\mathrm{sEMG_p(n)}$ can be acquired via the high-pass filter, low-pass filter and notch filter. However, in order to further eliminate jitter with huge amplitude, the full-wave rectification need to be applied to process the $\mathrm{sEMG_p(n)}$, the specific formula can be expressed as

$$\mathrm{sEMG}_r(n) = \left|\mathrm{sEMG}_p(n)\right| \tag{1}$$

where $\mathrm{sEMG_r(n)}$ is the nth amplitude sample of the sEMG signals obtained after full-wave rectification. In addition, on account of the sampling frequency of WT901C485 is 100HZ, which does not match the sampling frequency 2KHZ of MP160. Thus, the $\mathrm{sEMG_r(n)}$ will be sub-sampled to keep pace with the sampling frequency of WT901C485, the sub-sampled formula can be described as follows.

$$\mathrm{sEMG}_s(n) = \frac{1}{N}\sum_{i=nN-N+1}^{nN}\mathrm{sEMG}_r(i) \tag{2}$$

where N is the number of sub-sampling, and $\mathrm{sEMG_s(n)}$ is the sEMG signals after sub-sampling. Then, the processed signals $\mathrm{sEMG_s(n)}$ are revealed in Fig. 5

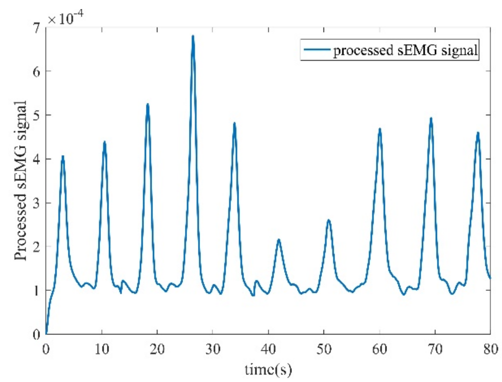

Fig. 5. The processed sEMG signal via high-pass filter, low-pass filter, notch filter, full-wave rectification and sub-sampling.

III. AFNN ESTABLISHMENT

Based on the fuzzy neural network, parameter optimization and sEMG signals, AFNN is established and applied to estimate the elbow joint angle. As can be seen from Fig. 6, specifically, the structure of fuzzy neural network consists of input layer, membership function, fuzzy rules and output layer. Thereinto, the data of actual elbow joint angle and processed sEMG signal can be expressed as

$$\begin{cases} \theta_a = \left[\theta_1,\ldots,\theta_j,\ldots,\theta_t\right] & t = 8000 \\ x = \left[x_1,\ldots,x_2,\ldots,x_t\right] & t = 1,\ldots,k \end{cases} \tag{3}$$

where θ_a is the actual elbow joint angle collected by WT901C485, and x signifies the processed sEMG signal. It is worth mentioning that the processed sEMG signal $x = [x_1, x_2, \ldots, x_{4000}]$ will be utilized as model intput. Accordingly, the output of AFNN is the estimated elbow joint angle θ_e. The membership function consists of numerous nodes ψ_{ij}, which indicates the j membership function of x_t, and R_L means the different combinations of fuzzy rules. Therefore, the formula of AFNN can be expressed as follows.

$$\theta_e = y = \sum_{j=1}^{L} \omega_j \psi_j \left(\frac{\| \vec{x} - \overrightarrow{\mu_j} \|}{\overrightarrow{\sigma_j}}\right) \tag{4}$$

where θ_e is the estimated elbow joint angle, respectively, $\overrightarrow{\sigma_j}$ signifies the variance of membership function, ω_j denotes the weight of ψ_j, and μ_j is the center of the membership function. In addition, the gaussian membership function ψ_j will be utilized to establish the AFNN, the formula can be described as

$$\psi_j = e^{-(\frac{x_i - \mu_{ij}}{\sigma_j})^2} \tag{5}$$

$$\mu_{ij} = \frac{1}{1 + e^{(\frac{b_{ij}x_{ij}+c_{ij}}{\sigma_{ij}})^2}} \tag{6}$$

then, combining the formula (4), (5) and (6), the formula (4) can be rewritten as

$$\theta_e = y = \frac{\sum_{j=1}^{L} \omega_j \Pi_{i=1}^{d_j} e^{-(\frac{x_i - \mu_{ij}}{\sigma_{ij}})^2}}{\sum_{j=1}^{L} \Pi_{i=1}^{d_j} e^{-(\frac{x_i - \mu_{ij}}{\sigma_{ij}})^2}} \quad 1 \le d_j \le D \tag{7}$$

where d_j and D respectively represent the dimension of ψ_j and input layer.

As can be seen from Fig. 7, the flowchart of elbow joint angle estimation consists of sEMG preprocessed, AFNN establishment and training, and AFNN parameters optimization and prediction. Firstly, the collected sEMG signal needs to be filtered. Secondly, AFNN needs parameter initialization, and then the filtered sEMG signal is passed as input to the fuzzification layer. Thirdly, the estimated elbow joint angle will be obtained via the fuzzy rule. It is worth mentioning that the parameters will be further optimized to update the layer of membership function and fuzzy rules via the error comparison. Ultimately, the optimal elbow joint estimation result will be output. In addition, in order to reveal the accuracy of the model prediction, the RMS error will be utilized to calculate the accuracy of the model. Specifically, in this experiment, the RMS formula can be expressed as

$$\text{RMS} = \sqrt{\frac{\sum_{i=1}^{4000}(\theta_a(i) - \theta_e(i))}{4000}} \tag{8}$$

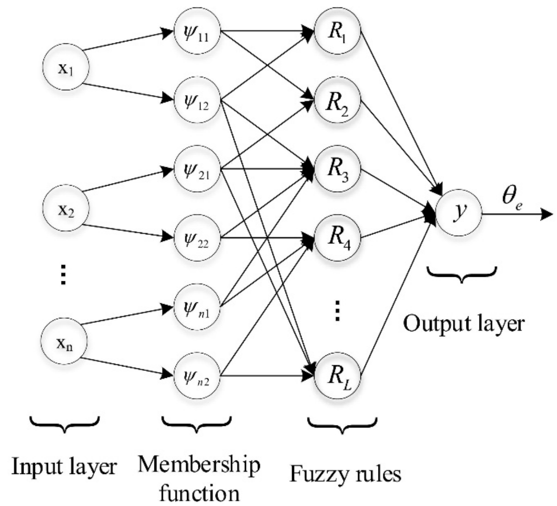

Fig. 6. The structural block diagram of AFNN.

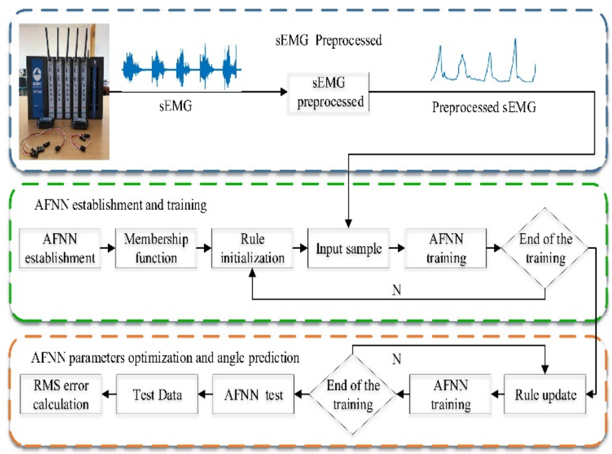

Fig. 7. The AFNN flowchart of elbow joint angle estimation.

IV. RESULT ANALYSIS

In this section, the AFNN based on the sEMG signals will be utilized to estimate the angle of elbow joint. For comparison, the BPNN and RBFNN will also be applied in this experiment, and the RMS error will illustrate the accuracy of AFNN, BPNN and RBFNN.

A. Experiments on AFNN

Based on the sEMG signals, the AFNN is employed to estimate the elbow joint angle, the result of estimated elbow joint angle (EEJA) and actual elbow joint angle (AEJA) can be seen in Fig. 8. Specifically, the red curve EEJA will approximate the blue curve AEJA with a small error in Fig. 8. As shown in Table.I, the AFNN will predict the elbow joint angle in 1.42s, and the RMS error reaches 9.1948 degree. The simulation results illustrate that AFNN is effective in elbow joint prediction.

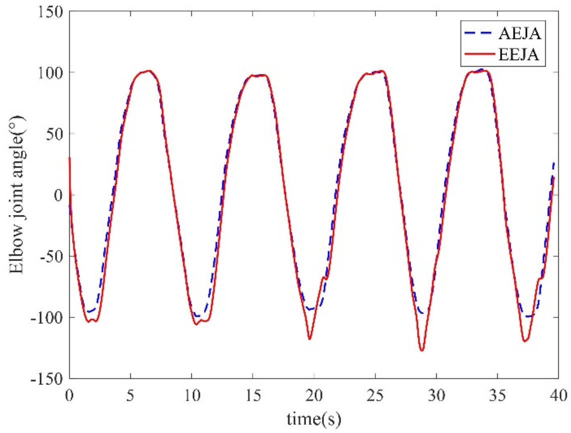

Fig. 8. The elbow joint angle estimated by AFNN.

B. Model comparison

In this subsection, the BPNN and RBFNN will be utilized to compare with AFNN in the estimation of elbow joint angle. In [14] and [15], the optimal parameters of hidden layer neurons and input order have been discussed in the human lower limb joint angle estimation. Therefore, the optimal parameters of hidden layer neurons $N_h = 20$ and input order $N_o = 20$ are set in this experiment. Correspondingly, the elbow joint angle estimated by BPNN and RBFNN are revealed in Fig. 9 and Fig. 10, and the RMS error of BPNN and RBFNN are shown in Table.I.

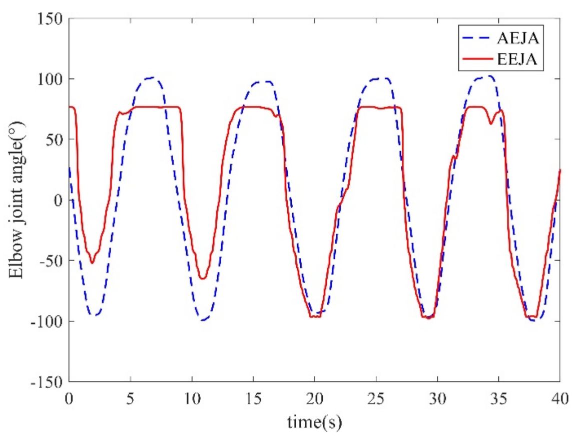

Fig. 9. The elbow joint angle estimated by BPNN with $N_h = 20$ and $N_o = 20$.

As can be seen from the Fig. 9, Fig. 10 and Table.I. Respectively, from the accuracy perspective, the BPNN with $N_h = 20$ and $N_o = 20$ estimates the elbow joint angle with large RMS error of 30.67 degree. However, BPNN has a larger RMS error in estimating the elbow joint angle at the peak of each cycle. That is to say, AFNN is superior to BPNN in estimated results at the end or the beginning of the human upper limb movement. Similarly, the EEJA of RBFNN with $N_h = 20$ and $N_o = 20$ approximates the AEJA with a large

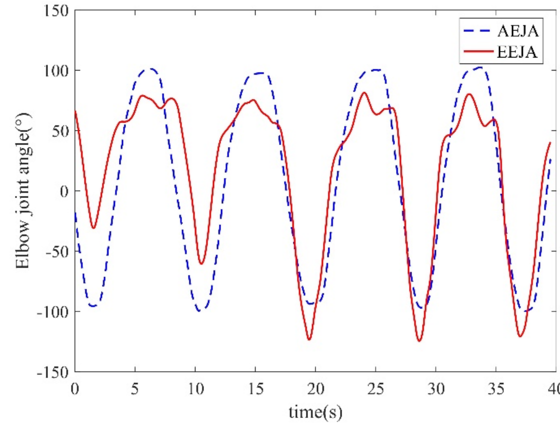

Fig. 10. The elbow joint angle estimated by RBFNN with $N_h = 20$ and $N_o = 20$.

TABLE I. COMPARISONS OF SIMULATION TIME AND RMS ERROR OF AFNN, BPNN AND RBFNN.

	AFNN	BPNN	RBFNN
RMS(∘)	9.19	30.67	39.21
time(s)	1.42	4.06	8.87

RMS error 39.21 degree in [0, 10]s, and the RBFNN is inferior to the AFNN at the peak of the cycle. From the rapidity perspective, although different parameters will lead to different experimental times, it will also produce the estimated results with different errors. Therefore, in the condition of optimal parameters, the running time of AFNN is much shorter than that of BNPP and RBFNN. In summary, the simulation results manifest that AFNN is superior to BPNN and RBFNN in terms of accuracy and rapidity.

V. CONCLUSIONS

In this paper, the AFNN based on the sEMG signals has been proposed, analyzed and investigated for estimating the elbow joint angle in comparison with the BPNN and RBFNN. The simulation results in Fig. 8, Fig. 9, Fig. 10 and Table. I have proved that the AFNN is superior to the BPNN and RBFNN in terms of accuracy and rapidity. Thereinto, the RMS error of AFNN is 3.3-4.3 times smaller than the one generated by BPNN and RBFNN, then, the simulation time of AFNN is still 2.8-6.2 times less than the simulation time of BPNN and RBFNN. Ultimately, the analysis of the rapidity and accuracy demonstrated that AFNN is superior to BPNN and RBFNN in the estimation of elbow joint angle.

For the future direction, the raw sEMG signals of anterior deltoid muscle, posterior deltoid muscle triceps muscle, biceps muscle, flexor carpi radialis and extensor carpi radialis will be collected from the spinal cord injury and stroke patients, then, the multiple joint angles of shoulder, elbow and wrist will be estimated by AFNN based on multi-channel sEMG signals. And then, based on the intention recognition of human, the human-robot interaction control algorithms based on neural network [22-24] will be designed to control the exoskeleton robot for assisting patients with rehabilitation training [21], so as to achieve the purpose of rehabilitation robot [25-27] to help the affected limb to perform rehabilitation training.

ACKNOWLEDGMENT

The authors would like to thank the editors and anonymous reviewers for their valuable suggestions and constructive comments which have really helped them improve very much the presentation and quality of the paper.

REFERENCES

[1] R. D. Zorowitz, P. J. Gillard and M. Brainin, "Poststroke spasticity: Sequelae and burden on stroke survivors and caregivers," Neurology, vol. 80, no. 3, pp. S45-S52, Jan. 2013.

[2] Z. J. Li, Z. C. Huang, W. He and C. Y. Su, "Adaptive Impedance Control for an Upper Limb Robotic Exoskeleton Using Biological Signals," IEEE Trans. Ind. Electron., vol. 64, no. 2, pp. 1664‑1674, Feb. 2017.

[3] X. Li, Y. P. Pan, G. Chen and H. Y. Yu, "Adaptive Human-Robot Interaction Control for Robots Driven by Series Elastic Actuators," IEEE Trans. Robot., vol. 33, no. 1, pp. 169-182, Feb. 2017.

[4] T. Y. Chen, R. Casas and P. S. Lum, "An Elbow Exoskeleton for Upper Limb Rehabilitation With Series Elastic Actuator and Cable-Driven Differential," IEEE Trans. Robot., vol. 35, no. 6, pp. 1464-1474, Dec. 2019.

[5] Z. J. Li, C. Y. Su, G. L. Li and H. Su, "Fuzzy Approximation-based Adaptive Backstepping Control of an Exoskeleton for Human Upper Limbs," IEEE Trans. Fuzzy Syst., vol. 23, no. 3, pp. 555-566, Apr. 2015.

[6] J. H. Han, S. J. Lee and J. H. Kim, "Behavior hierarchy-based affordance map for recognition of human intention and its application to human-robot interaction," IEEE Trans. Hum.-Mach. Syst., vol. 46, no. 5, pp. 708-722, May. 2016.

[7] Y. Nam, B. Koo, A. Cichocki and S. Choi, "GOM-Face: GKP, EOG, and EMG-Based Multimodal Interface With Application to Humanoid Robot Control," IEEE Trans. Biomed. Eng., vol. 61, no. 2, pp. 453-462, Sep. 2013.

[8] F. Duan, L. L. Dai, W. N. Chang, Z. Q. Chen, C. Zhu and W. Li, "SEMG-based identification of hand motion commands using wavelet neural network combined with discrete wavelet transform," IEEE Trans. Ind. Electron., vol. 63, no. 3, pp. 1923-1934, Nov. 2015.

[9] L. Jin, S. Li, J. G. Yu and J. B. He, "Robot manipulator control using neural networks: a survey," Neurocomputing, vol. 285, no. 12, pp. 23-24, Apr. 2018.

[10] Z. B. Sun, F. Li, B. C. Zhang, Y. Y. Sun and L. Jin, "Different modified zeroing neural dynamics with inherent tolerance to noises for time-varying reciprocal problems: A control-theoretic approach," Neurocomputing, vol. 337, pp. 165-179, Apr. 2019.

[11] Z. B. Sun, Y. B. Liu, L. Wei, K. P. Liu, L. Jin and L. Q. Ren, "Two DTZNN Models of O(τ^4) Pattern for Online Solving Dynamic System of Linear Equations: Application to Manipulator Motion Generation," IEEE Access, vol. 8, pp. 36624-36638, Feb. 2020.

[12] J. Shi, Y. P. Zheng and Z. Z. Yan, "SVM for estimation of wrist angle from sonomyography and sEMG signals," IEEE International Conference on EMBS, pp. 4806-4809, Oct. 2007.

[13] B. W. Gao and W. L. Han, "Neural network model reference decoupling control for single leg joint of hydraulic quadruped robot," Assem. Autom., vol. 38, no. 4, pp. 465-475, Sep. 2018.

[14] F. Zhang, P. F. Li, Z. G. Hou, Z. Lu, Y. X. Chen, Q. L. Li and M. Tan, "sEMG-based continuous estimation of joint angles of human legs by using BP neural network," Neurocomputing, vol. 78, no. 1, pp. 139-148, Feb. 2012.

[15] G. Wang, Y. B. Liu, T. Shi, X. Q. Duan, K. P. Liu, Z. B. Sun and L. Jin, "A Novel Estimation Approach of sEMG-based Joint Movements via RBF Neural Network," 2019 Chinese Automation Congress, pp. 2059-2064, Feb. 2020.

[16] M. Yoshikawa, M. Mikawa and K. Tanaka, "Hand Pose Estimation Using EMG Signals," IEEE International Conference on EMBS, pp. 4830-483, 2007.

[17] Z. B. Sun, F. Li, G. Wang, Y. B. Liu, Y. F. Lian and K. P. Liu, "A Novel RBF Neural Network-Based Iterative Learning Control For Lower Limb Rehabilitation Robot With Strong Robustness," 2019 Chinese Control Conference, pp. 4445-4450, Oct. 2019.

[18] Y. Y. Chai, K. P. Liu, Z. B. Sun, G. Wang and T. Shi, "A long short term memory network based on surface electromyography for continuous estimation of elbow joint angle," 2020 IEEE 9th Data Driven Control and Learning Systems Conference, unpublished.

[19] A. van Boxtel, A. J. W. Boelhouwer and A. R. Bos, "Optimal EMG signal bandwidth and interelectrode distance for the recording of acoustic, electrocutaneous, and photic blink reflexes," Psychophysiology, vol. 35, no. 6, pp. 690-697, Nov. 1998.

[20] A. Christie, I. J. Greig, G. Kamen and D. A. Gabriel, "Relationships between surface EMG variables and motor unit firing rates," Eur. J. Appl. Physiol., vol. 107, no. 2, pp. 177-185, Jun. 2009.

[21] J. Zhang, P. Fiers, K. A. Witte, R. W. Jackson, K. L. Poggensee, C. G. Atkeson, and S. H. Collins, "Human-in-the-loop optimization of exoskeleton assistance during walking," Science, vol. 356, no. 6344, pp. 1280‑1284, Jun. 2017.

[22] Z. Sun, F. Li, B. Zhang, Y. Sun, and L. Jin, "Different modified zeroing neural dynamics with inherent tolerance to noises for time-varying reciprocal problems: A control-theoretic approach," Neurocomputing, vol. 337, pp. 165‑179, Apr. 2019.

[23] L. Jin, J. Yan, X. Du, X. Xiao, and D. Fu, "RNN for solving time-variant generalized Sylvester equation with applications to robots and acoustic source localization," IEEE Trans Ind. Informat., to be published, doi: 10.1109/tii.2020.2964817.

[24] Z. Sun, T. Shi, L. Wei, Y. Sun, K. Liu, and L. Jin, "Noise-suppressing zeroing neural network for online solving time-varying nonlinear optimization problem: A control-based approach," Neural Comput. Appl., Dec. 2019, doi: 10.1007/s00521-019-04639-2.

[25] A. S. Niyetkaliyev, S. Hussain, M. H. Ghayesh and G. Alici, "Review on Design and Control Aspects of Robotic Shoulder Rehabilitation Orthoses," IEEE T. Hum.-Mach. Syst., vol. 47, no. 6, pp. 1134-1145, May. 2017.

[26] E. T. Wolbrecht, V. Chan, D. J. Reinkensmeyer and J. E. Bobrow, "Optimizing Compliant, Model-Based Robotic Assistance to Promote Neurorehabilitation," IEEE Trans. Neural Syst. Rehabil. Eng., vol. 16, no. 3, pp. 286-297, Jun. 2008.

[27] Z. Li, C.-Y. Su, L. Wang, Z. Chen, and T. Chai, "Nonlinear disturbance observer design for a robotic exoskeleton incorporating fuzzy approximation," IEEE Trans. Ind. Electron., vol. 62, no. 9, pp. 5763-5775, Sep. 2015.